An HLLC Riemann Solver for Magnetohydrodynamics

Shengtai Li

Theoretical Division, MS B284, Los Alamos National Laboratory, Los Alamos, NM 87545

Abstract

This paper extends a class of approximate Riemann solvers devised by Harten, Lax and van Leer (HLL) for Euler equations of hydrodynamics to magneto-hydrodynamics (MHD) equations. In particular, we extend the two-state HLLC (HLL for contact wave) construction of Toro, Spruce and Speares to MHD equations. We derive a set of HLLC middle states that satisfies the conservation laws. Numerical examples are given to demonstrate that the new MHD-HLLC solver can achieve high numerical resolution, especially for resolving contact discontinuity. In addition, this new solver maintains a high computational efficiency when compared to Roe's approximate Riemann solver.

Key words: approximate Riemann solver, HLL, HLLE, HLLC, magneto-hydrodynamics (MHD)

1 Introduction

Many astrophysics problems demand solutions of magneto-hydrodynamics (MHD) equations. There are many numerical techniques to solve MHD equations. In this paper, we consider a Godunov type of method. Godunov's method and its various derivatives have gained increasing popularity in solving the Euler equations of hydrodynamics (HD) due to their robustness and ability to achieve high resolution near discontinuities. Central to these methods is the exact or approximate solutions of the Riemann problem. In the last decade, several Godunov methods for HD have been extended to MHD systems. These methods conservatively update the zone-averaged or grid-centered fluid and magnetic field quantities based on estimated advective fluxes of mass, momentum, energy and magnetic field at grid interfaces using solutions to the Riemann problem at interfaces. Some of the MHD examples have been given

Email address: sli@lanl.gov (Shengtai Li).

by Brio and Wu [5], Zachary et al. [26]. Dai and Woodward [7,8], Powell [17], Ryu and Jones [21], Roe and Balsara [20], and Balsara [2], among others.

The exact Riemann solver is generally considered too expensive for most Godunov type methods. As a result, several approximate Riemann solvers have been developed. One of the most widely used solvers is the Roe's approximate Riemann solver [19], which has been applied to MHD by many authors (see [5,17,21,20,2,18]). Roe's solver requires eigen-decomposition, which becomes more complicated and time-consuming in MHD than in HD [20]. Moreover, Roe's approximate Riemann solver does not preserve the positivity [10]. This problem becomes worse in MHD when gas pressure is much less than magnetic pressure.

The approximate Riemann solver devised by Harten, Lax, and van Leer [12] (HLL) has a nice property that it is a positive scheme if used with an appropriate choice of wavespeed bounds for any conservative hyperbolic system. The HLL Riemann solver does not require field-decomposition. The simple single state HLL solver assumes only one intermediate wave state between the two acoustic waves and has been shown to be reliable and robust in most applications. A typical example of the single state HLL solver is HLLE scheme by Einfeldt et al. [10], who proposed a particular wavespeed bound which enables the intermediate state to satisfy the so-called entropy and positivity conditions.

The single-state HLL and HLLE solvers, however, are too diffusive and cannot resolve isolated contact discontinuities very well. In the original work by Harten et al. [12], they have already realized this problem and suggested that a two-state approximation could yield an exact resolution of an isolated intermediate wave (e.g., a shock, contact, or Alfvén wave, etc). They further proposed a general framework to construct such types of solvers. The full implementation of this approach, however, was never given, perhaps partly owing to the fact that the two-state HLL algorithm described in [12] is non-intuitive, cumbersome and somewhat ambiguous because it contains arbitrary constants [15]. Another approach to improve the single-state HLL scheme was introduced in Ref. [10], called HLLEM. This approach used a partial eigen-decomposition and added anti-diffusion terms only to the linearly-degenerated fields.

A different but much simpler approach in constructing the two-state HLL-type solvers came from Toro et al. [24], who assumed that the intermediate left and right states have the same velocity and pressure. These assumption are physically valid for the contact wave, which is why this solver is called HLLC ("C" stands for *Contact*). Batten et al. [4] retained the basic assumptions of Toro et al. but suggested a different way for computing the wavespeed of the intermediate states. They showed that their HLLC solver can resolve isolated shock and contact waves exactly and remain positively conservative for HD equations with a proper choice of the wavespeed bounds.

Recently, Linde [15] proposed a new, general purpose, two-state HLL solver by following the original two-state framework by Harten et al. [12], though his method is substantially simpler. The two-state HLL solver is based on a convex entropy function, its gradients and Hessian matrix to identify the velocity and strength of the middle wave. Linde used a geometric interpretation of the Rankine-Hugoniot conditions to estimate the speed and strength of the

middle wave, therefore eliminating the arbitrary constants of the original HLL framework.

Many of the HLL-type solvers discussed above have been applied to MHD problems with varying degree of success. Examples include Janhunen [13], Wesenberg [25], Linde [15], Gurski [11], and others. Motivated by the work of Powell [17], Janhunen [13] developed a new MHD-HLL scheme while adding a source term proportional to $\nabla \cdot \mathbf{B}$ in the induction equation. He then showed by extensive tests that no counterexamples have been found to the positivity of this MHD-HLL method. Wesenberg [25] extended HLLEM to MHD by adding anti-diffusion terms to all the waves except the two fast magneto-sonic waves. He then demonstrated numerically that for both smooth and non-smooth problems in 1D and 2D, MHD-HLLEM was the most efficient solver in terms of computational time versus error. Since MHD flows contain as many as seven (or eight) eigen-waves, however, the computational saving by HLLEM over the Roe's solver may not be as great as that in the pure HD flows. The solver developed by Linde [15] is directly applicable to MHD problems and has been shown to be better than the HLLE solver. Some recent studies aimed at applying HLLC to MHD problems (e.g., Gurski [11]). However, we found that a straightforward implementation of Toro and Batten's HLLC solver for MHD equations failed and/or yielded unphysical solutions which violate conservation laws.

In this paper, we propose a new MHD-HLLC solver which is the same as Toro and Batten's HLLC solver in the pure HD limit but satisfies the conservation laws in MHD. The outline of the paper is as follows. In Section 2, we review the HLL and HLLC solvers for HD equations. In Section 3, we derive the new MHD-HLLC solver for MHD, first for 1-D and then for multi-dimensional problems. Several examples are given in Section 4, demonstrating the effectiveness of our scheme.

2 HLL and HLLC Riemann solver for HD

For the sake of completeness and ease of subsequent discussion on how to build a new MHD-HLLC solver, we will first give a brief overview on the construction of HLL and HLLC solvers for pure HD.

2.1 The HLL flux

The Euler equations may be written as

$$\frac{\partial \mathbf{U}}{\partial t} + \nabla \cdot F(\mathbf{U}) = 0, \tag{1}$$

where $\mathbf{U}$ and $F(\mathbf{U})$ represent the conservative variables and their fluxes,

$$\mathbf{U} = \begin{bmatrix} \rho \\ \rho\mathbf{u} \\ E \end{bmatrix}, \quad F(\mathbf{U}) = \begin{bmatrix} \rho\mathbf{u} \\ \rho\mathbf{u}\mathbf{u}^T + p\mathbf{I} \\ (E+p)\mathbf{u} \end{bmatrix},$$

where $\rho, \mathbf{u} = (u, v, w), E$ and p represent density, Cartesian velocity components, total energy per unit volume, and pressure, respectively.

Consider the Riemann problem along the x-direction, it has the following piece-wise constant initial data for the left and right states

$$\mathbf{U}(x, 0) = \begin{cases} \mathbf{U}_l, & \text{if } x < 0, \\ \mathbf{U}_r, & \text{if } x > 0. \end{cases}$$

A simple conservative discretization for Eq. (1) gives

$$\mathbf{U}_i^{n+1} = \mathbf{U}_i^n - \frac{\Delta t}{\Delta x}(F_{i+\frac{1}{2}} - F_{i-\frac{1}{2}}).$$

In the HLL approach, to calculate the fluxes $F_{i+\frac{1}{2}}$, Harten, Lax and van Leer [12] proposed a single state approximate Riemann solution as

$$\mathbf{U}_{HLL} = \begin{cases} \mathbf{U}_l, & \text{if } S_L > 0, \\ \mathbf{U}^*, & \text{if } S_L \leq 0 \leq S_R, \\ \mathbf{U}_r, & \text{if } S_R < 0. \end{cases}$$

where S_L and S_R represent the fastest wave speed for the left and right states, respectively. The variable $\mathbf{U}^*$ denotes the intermediate subsonic state and is defined as

$$\mathbf{U}^* = \frac{S_R\mathbf{U}_r - S_L\mathbf{U}_l - (F_r - F_l)}{S_R - S_L}, \tag{2}$$

where $F_l = F(\mathbf{U}_l)$ and $F_r = F(\mathbf{U}_r)$. The corresponding interface flux is defined as

$$F_{HLL} = \begin{cases} F_l, & \text{if } S_L > 0, \\ F_{lr}, & \text{if } S_L \leq 0 \leq S_R, \\ F_r, & \text{if } S_R < 0 \end{cases}$$

where F_{lr} is given as

$$F_{lr} = \frac{S_R F_l - S_L F_r + S_L S_R(\mathbf{U}_r - \mathbf{U}_l)}{S_R - S_L}.$$

Note that $F_{HLL} \neq F(\mathbf{U}_{HLL})$ for the subsonic case $S_L \leq 0 \leq S_R$.

There are several methods to evaluate the wavespeed bounds S_L and S_R [23] and in this paper, we adopt the one proposed in [10] because they have shown, with their choices of S_L and S_R, the HLL Riemann solver satisfies an entropy inequality, resolves isolated shocks exactly and preserves positivity [10].

The HLLC flux is a modification of F_{HLL}. Instead of a single intermediate state $\mathbf{U}^*$, two intermediate states, $\mathbf{U}_l^*$ and $\mathbf{U}_r^*$, are assumed, separated by an interface moving with speed S_M. To calculate $\mathbf{U}_l^*$ and $\mathbf{U}_r^*$, we recap the approach taken by Batten et al. by applying the Rankine-Hugoniot conditions across the S_L wave

$$F_l^* = F_l + S_L(\mathbf{U}_l^* - \mathbf{U}_l). \tag{3}$$

Similarly, the jump relation across the S_R wave gives,

$$F_r^* = F_r + S_R(\mathbf{U}_r^* - \mathbf{U}_r). \tag{4}$$

Equation (3) may be rewritten as

$$S_L\mathbf{U}_l^* - F_l^* = S_L\mathbf{U}_l - F_l. \tag{5}$$

Following Batten et al. and assuming $F_l^* = F(U_l^*)$, we can write out Eq. (5) along the direction $\vec{n} = (n_x, n_y, n_z)$ which is normal to the interface separating states U_l and U_l^*,

$$S_L \begin{bmatrix} \rho_l^* \\ \rho_l^* u_l^* \\ \rho_l^* v_l^* \\ \rho_l^* w_l^* \\ E_l^* \end{bmatrix} - \begin{bmatrix} \rho_l^* q_l^* \\ \rho_l^* u_l^* q_l^* + p^* n_x \\ \rho_l^* v_l^* q_l^* + p^* n_y \\ \rho_l^* w_l^* q_l^* + p^* n_z \\ (E_l^* + p^*) q_l^* \end{bmatrix} = S_L \begin{bmatrix} \rho_l \\ \rho_l u_l \\ \rho_l v_l \\ \rho_l w_l \\ E_l \end{bmatrix} - \begin{bmatrix} \rho_l q_l \\ \rho_l u_l q_l + p n_x \\ \rho_l v_l q_l + p n_y \\ \rho_l w_l q_l + p n_z \\ (E_l + p) q_l \end{bmatrix} \tag{6}$$

where $q_l = u_l n_x + v_l n_y + w_l n_z$ is the velocity component of the state U_l along $\vec{n}$. q_l^* is defined similarly.

Toro, Spruce, and Speares [24] made the further assumption that the wavespeed is constant between the two acoustic waves,

$$S_M = q_l^* = q_r^* = q^*.$$

Eq. (6) shows that the $\mathbf{U}_{l,r}^*$ can be solved uniquely if q^* and $\mathbf{U}_{l,r}$ are known.

There are several approaches to estimate the middle wave speed q^* (see Ref. [24]). We used an approach proposed by Batten et al. [4]. This approach is to extract the average velocity q^* from the HLL approximation of $\mathbf{U}^*$. Taking the Riemann problem in x-direction as an example, $\vec{n} = (1, 0, 0), q = u$, we have

$$q^* = \frac{\rho_r q_r(S_R - q_r) - \rho_l q_l(S_L - q_l) + p_l - p_r}{\rho_r(S_R - q_r) - \rho_r(S_L - q_l)}. \tag{7}$$

3 HLLC for MHD

3.1 Eigen structure for MHD

The ideal MHD equations can be formulated as

$$\rho_t + \nabla \cdot (\rho \mathbf{u}) = 0, \tag{8}$$
$$(\rho \mathbf{u})_t + \nabla \cdot \left[\rho \mathbf{u}\mathbf{u}^T + (p)\mathbf{I} - \mathbf{B}\mathbf{B}^T\right] = 0, \tag{9}$$
$$E_t + \nabla \cdot [(E+p)\mathbf{u} - \mathbf{B}(\mathbf{u}\cdot\mathbf{B})] = 0, \tag{10}$$
$$\mathbf{B}_t - \nabla \cdot (\mathbf{u}\mathbf{B}^T - \mathbf{B}\mathbf{u}^T) = 0, \tag{11}$$

where ρ is density, $\mathbf{u}$ is the velocity, $\mathbf{B}$ is the magnetic field, E is the total energy per unit volume, and p is the total pressure, defined as

$$p = p_{\text{gas}} + \frac{1}{2}\mathbf{B}\cdot\mathbf{B}, \tag{12}$$

where p_{gas} is the gas pressure that satisfies the equation of state,

$$p_{\text{gas}} = (\gamma - 1)\left(E - \frac{1}{2}\rho\mathbf{u}\cdot\mathbf{u} - \frac{1}{2}\mathbf{B}\cdot\mathbf{B}\right).$$

One external constraint for magnetic field is the *divergence-free* condition $\nabla \cdot \mathbf{B} = 0$, which becomes $B_x =$ constant in one dimension.

Figure 3.1 shows the $\{x - t\}$ diagram of all the waves at a cell interface for MHD. They are: one entropy waves with speed u, two Alfvén waves with speed $u \pm c_a$, where $c_a = B_x/\sqrt{\rho}$, and four magneto-acoustic waves (two fast and two slow) with speed, $u \pm c_f$ and $u \pm c_s$, where

$$c_{f,s}^2 = \frac{1}{2}\left(\frac{\gamma p + \mathbf{B}\cdot\mathbf{B}}{\rho} \pm \sqrt{\left(\frac{\gamma p + \mathbf{B}\cdot\mathbf{B}}{\rho}\right)^2 - 4\frac{\gamma p B_x^2}{\rho^2}}\right),$$

and "+" for fast and "-" for slow waves.

3.2 HLLC for 1-D MHD

For simplicity, we consider the ideal MHD equations in Cartesian grids only. It can be readily applied to other orthogonal curvilinear grids. We first show that a straightforward extension of HLLC scheme of [24] to the MHD equations does not work. Then we propose our modified MHD-HLLC scheme.

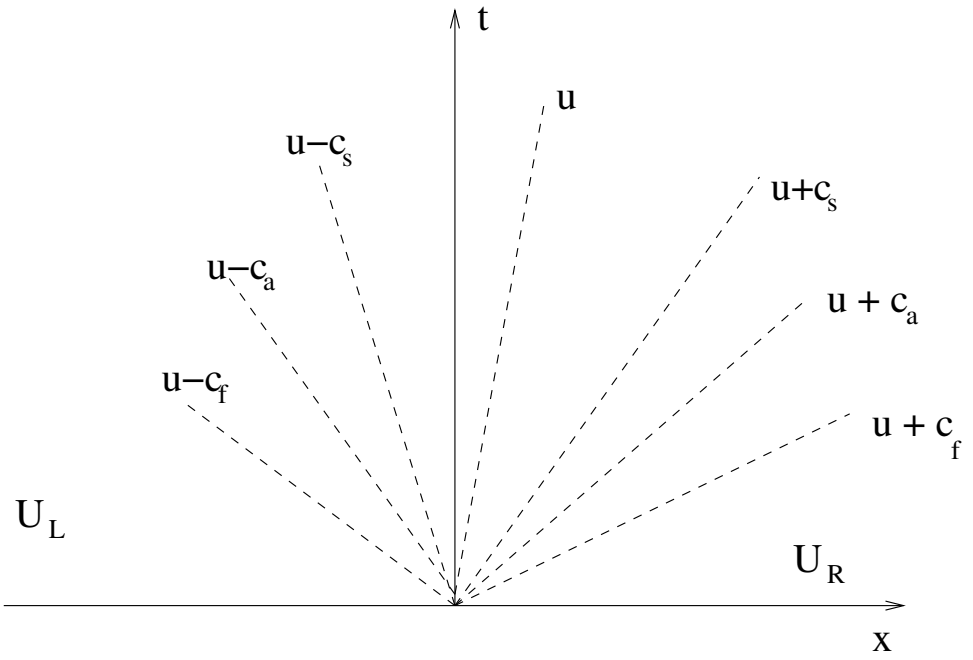

Fig. 3.1. Waves in 1-D MHD Riemann problem.

Consider the 1-D MHD equations, where B_x is constant. Re-write Eq. (6) for MHD, we get (subscript l is dropped for simplicity)

$$S_L \begin{bmatrix} \rho^* \\ \rho^* u^* \\ \rho^* v^* \\ \rho^* w^* \\ B_x^* \\ B_y^* \\ B_z^* \\ E^* \end{bmatrix} - \begin{bmatrix} \rho^* q^* \\ \rho^* u^* q^* + p^* - (B_x^*)^2 \\ \rho^* v^* q^* - B_x^* B_y^* \\ \rho^* w^* q^* - B_x^* B_z^* \\ 0 \\ u^* B_y^* - v^* B_x^* \\ u^* B_z^* - w^* B_x^* \\ (E^* + p^*) q^* - B_x^* (\mathbf{B} \cdot \mathbf{u})^* \end{bmatrix} = S_L \begin{bmatrix} \rho \\ \rho u \\ \rho v \\ \rho w \\ B_x \\ B_y \\ B_z \\ E \end{bmatrix} - \begin{bmatrix} \rho q \\ \rho u q + p - (B_x)^2 \\ \rho v q - B_x B_y \\ \rho w q - B_x B_z \\ 0 \\ u B_y - v B_x \\ u B_z - w B_x \\ (E + p) q - B_x (\mathbf{B} \cdot \mathbf{u}) \end{bmatrix}, \quad (13)$$

where p (or p^*) represents the total pressure, defined by (12), and $u^* = q^*$, $u = q$.

Similar to Eq. (7), the speed q^* for MHD can be written as

$$q^* = \frac{\rho_r q_r (S_R - q_r) - \rho_l q_l (S_L - q_l) + p_l - p_r - B_{x_l}^2 + B_{x_r}^2}{\rho_r (S_R - q_r) - \rho_r (S_L - q_l)}. \quad (14)$$

Other components of $\mathbf{U}^*$ can now be derived from Eq. (13). After some manipulation, we obtain

$$B_y^* = \frac{(S_L - u - \frac{B_x^* B_x}{\rho (S_L - u)}) B_y - (B_x^* - B_x) v}{S_L - q^* - \frac{(B_x^*)^2}{\rho (S_L - u)}}, \quad (15)$$

$$B_z^* = \frac{(S_L - u - \frac{B_x^* B_x}{\rho(S_L-u)})B_z - (B_x^* - B_x)w}{S_L - q^* - \frac{(B_x^*)^2}{\rho(S_L-u)}}. \tag{16}$$

and

$$p^* = \rho(S_L - u)(q^* - u) + p - B_x^2 + (B_x^*)^2. \tag{17}$$

To satisfy the assumption $p_l^* = p_r^*$ with the definition of q^*, we obtain

$$B_{x_l}^* = B_{x_r}^*. \tag{18}$$

which is obviously true in 1D. We will re-visit this relation for multi-dimensional problems in Section 3.3. With the known values of B_x^*, B_y^*, B_z^*, q^* and p^*, the rest of the components can be derived easily:

$$\rho_l^* = \rho\frac{S_L - u}{S_L - q^*}, \tag{19}$$

$$(\rho u)_l^* = \rho^* q^*, \tag{20}$$

$$(\rho v)_l^* = (\rho v)\frac{S_L - u}{S_L - q^*} - \frac{(B_x^* B_y^* - B_x B_y)}{S_L - q^*}, \tag{21}$$

$$(\rho w)^* = (\rho w)\frac{S_L - u}{S_L - q^*} - \frac{(B_x^* B_z^* - B_x B_z)}{S_L - q^*}, \tag{22}$$

$$E_l^* = E\frac{S_L - u}{S_L - q^*} + \frac{(p^* q^* - pu) - (B_x^*(\mathbf{B}\cdot\mathbf{u})^* - B_x(\mathbf{B}\cdot\mathbf{u}))}{S_L - q^*}. \tag{23}$$

The right middle state $\mathbf{U}_r^*$ can be derived similarly. The two-state HLLC fluxes can be calculated via Eqs. (3) and (4).

Unfortunately, the HLLC middle state $\mathbf{U}^*$ derived above is not consistent with the integral form of the conservation laws, which is described as a *Consistency Condition* by Toro [23]:

$$\frac{q^* - S_L}{S_R - S_L}\mathbf{U}_l^* + \frac{S_R - q^*}{S_R - S_L}\mathbf{U}_r^* = \frac{S_R\mathbf{U}_r - S_L\mathbf{U}_l - (F_r - F_l)}{S_R - S_L}, \tag{24}$$

even though the pure HD HLLC intermediate states do satisfy this condition. Indeed, when we tested the solution from Eqs. (15) to (23), we found that they either failed quickly or gave completely unphysical results.

However, we were able to find a set of solutions which complies with the conservation law Eq. (24) by the following procedure. We choose to keep Eqs. (14) and (17) unchanged. The idea is to see whether we can derive new expressions for B_y^* and B_z^* that satisfy Eq. (24).

Substituting Eqs. (21) and (22) into Eq. (24), we obtain the following conditions for the magnetic components

$$B^*_{x_l} B^*_{y_l} = B^*_{x_r} B^*_{y_r}, \tag{25}$$
$$B^*_{x_l} B^*_{z_l} = B^*_{x_r} B^*_{z_r}. \tag{26}$$

Since $B^*_{x_l} = B^*_{x_r}$ from condition (18), Eqs. (25) and (26) give

$$B^*_{y_l} = B^*_{y_r}, \quad B^*_{z_l} = B^*_{z_r}. \tag{27}$$

Furthermore, we assign the single HLL average state values to them using Eq. (2),

$$B^*_{y_l} = B^*_{y_r} = B^{HLL}_y, \quad B^*_{z_l} = B^*_{z_r} = B^{HLL}_z. \tag{28}$$

Note that other choices for B^*_y and B^*_z should also work as long as they satisfy Eq. (27).

Having derived the new B^*_y and B^*_z, along with q^* and p^*, we now proceed to find a new $E^*_{l,r}$, defined in (23), which satisfies Eq. (24). Substituting Eq. (23) into Eq. (24), we get

$$B^*_{x_l} (\mathbf{B}\cdot\mathbf{u})^*_l = B^*_{x_r} (\mathbf{B}\cdot\mathbf{u})^*_r, \quad \text{or} \quad (\mathbf{B}\cdot\mathbf{u})^*_l = (\mathbf{B}\cdot\mathbf{u})^*_r \ . \tag{29}$$

As in Eq. (27), we can assign the HLL average values to them,

$$(\mathbf{B}\cdot\mathbf{u})^*_l = (\mathbf{B}\cdot\mathbf{u})^*_r := \mathbf{B}^{HLL}\cdot\mathbf{u}^{HLL}, \tag{30}$$

and the middle state Eq. (23) becomes

$$E^*_l = E\frac{S_L - u}{S_L - q^*} + \frac{(p^*q^* - pu) - (B^*_x(\mathbf{B}^{HLL}\cdot\mathbf{u}^{HLL}) - B_x(\mathbf{B}\cdot\mathbf{u}))}{S_L - q^*}. \tag{31}$$

The quantity $\mathbf{u}^{HLL}$ can be calculated from the conservative variables $\mathbf{U}_{HLL}$. We remark that if we had chosen $(\mathbf{B}\cdot\mathbf{u})^*_k = \mathbf{B}^*_k\cdot\mathbf{u}^*_k$, Eq. (29) would not be satisfied by the given expressions of $\mathbf{B}^*$ and $\mathbf{u}^*$.

With the newly derived $\mathbf{U}^*_{l,r}$ that satisfy Eq. (24), we can now write the MHD-HLLC flux as, keeping the original format,

$$F_{HLLC} = \begin{cases} F_l, & \text{if } 0 \le S_L \\ F^*_l = F_l + S_L(\mathbf{U}^*_l - \mathbf{U}_l), & \text{if } S_L \le q^* \\ F^*_r = F_r + S_R(\mathbf{U}^*_r - \mathbf{U}_r), & \text{if } q^* \le S_R \\ F_r, & \text{if } 0 \ge S_R. \end{cases} \tag{32}$$

3.3 HLLC for multi-dimensional MHD

In keeping with the HLLC assumption that $p_l^* = p_r^*$, which results in the condition Eq. (18), we adopt a convenient extension into multi-dimensional cases by requiring

$$B_{x_l}^* = B_{x_r}^* = B_x^{HLL} = \frac{S_R B_{x_r} - S_L B_{x_l}}{S_R - S_L}. \tag{33}$$

Then the whole set of expressions for the intermediate states $\mathbf{U}_{l,r}^*$ described in the last section remains the same.

4 Numerical Experiment

In this section, we provide some examples to test our new MHD-HLLC solver. The dimensional split version of our solvers (see [16]) is used. The CFL number is set as 0.8 and time step is determined adaptively. To preserve the divergence-free constraint of magnetic fields, the flux-CT approach on staggered grid [1] is used. Whenever the cell-centered magnetic field components are needed, interpolations from the face-centered values are used.

4.1 Rotated shock-tube problem

The first test problem was introduced in Ref.[21] as a 1-D MHD Riemann problem. It was later used by Ref.[22] to compare several numerical schemes for MHD. We adopt the same initial and boundary conditions as in Ref.[22]. The initial left and right states are

$$(\rho, v_\parallel, v_\perp, v_z, p, B_\parallel, B_\perp, B_z) = \begin{cases} (1.08, 1.2, 0.01, 0.5, 0.95, \frac{2}{\sqrt{4\pi}}, \frac{3.6}{\sqrt{4\pi}}, \frac{2}{\sqrt{2\pi}}), & \text{left}, \\ (1, 0, 0, 0, 1, \frac{2}{\sqrt{4\pi}}, \frac{4}{\sqrt{4\pi}}, \frac{2}{\sqrt{2\pi}}), & \text{right}, \end{cases}$$

where $\parallel$ refers to the direction along the normal of the shock front, $\perp$ refers to the direction perpendicular to the normal of the shock front but still in the computational plane, and z refers to the direction out of the plane. It involves three-dimensional field and velocity structure where the magnetic field plane rotates. Since all of the three magnetic components are non-zero, it is often referred as a 2.5D problem.

The Riemann solution for this example contains two fast shocks, two rotational discontinuities, two slow shocks, and a contact discontinuity between the two slow shocks. As in [22], we solved it as an oblique shock-tube problem in 2-D. In [22], the angle between the shock interface and y-axes is set to 45 degree. To break the symmetry, we solved it with an angle of $\alpha = \tan^{-1} 2 \approx 63.4°$. Initial domain and problem set-up is the same as in [22] except that the local grid spacing is different. We use 400 cells in x-direction. The number

of cells in y-direction is equal to the number of ghost cells. In [22], $dy = dx$ was used, which leads to that the shock interface is not in a straight line and the parallel component of the magnetic field is not conserved as it should be even if the flux-CT is used. We modify the local spacing in y-direction so that the shock interface has a straight line. For $\alpha = \tan^{-1} 2$, we set $dy = dx/2$. After this modification, the parallel component of the magnetic field is conserved exactly if the flux-CT is used.

Figs. 4.1 and 4.2 show the results for $\alpha = 0$ and $\tan^{-1} 2$. For comparison, we also include the results of two-state HLL solver of Linde [15] for $\alpha = 0$. We can see that our MHD-HLLC greatly improves the results over the HLL solver. For this calculation, the HLL and MHD-HLLC took almost the same CPU time (4.102s vs. 4.215s), whereas the Roe's solver took 6.175 seconds.

To quantify the numerical error, we calculate an L_1 error as follows. First we obtain a reference solution of 400 cells by averaging the solutions of $N = 1600$ over each coarse cell. Then the difference Δu^i_j between the numerical solution and reference solution is computed. Finally, the total error is calculated as

$$Err = \sum_{i=1}^{N_u} \sum_{j=1}^{N} \frac{|\Delta u^i_j|}{\max\limits_j |u^i|}, \tag{34}$$

where u^i is only for the cell-centered variables. The errors of the four schemes (Roe's, MHD-HLLC, Linde's two-state HLL, and HLL) for $\alpha = 0$ are 0.0098, 0.0118, 0.0135, and 0.0148, respectively.

The next shock-tube problem is originally from Brio and Wu [5], which is a classical test problem for ideal MHD codes. It is a 1-D shock-tube problem with the initial states

$$(\rho, v_\parallel, v_\perp, p, B_\perp, B_z, p) = \begin{cases} (1, 0, 0, 0, 1, 0, 1), & \text{left,} \\ (0.125, 0, 0, 0, -1, 0, 0.1), & \text{right.} \end{cases}$$

and $B_\parallel = 0.75$. Again we solved it as a fully 2-D problem with an angle α between the shock interface and y-axes. The 2D test with $\alpha = 45^\circ$ has been solved by Jiang and Wu [14], and many others. We solved it with $\alpha = \tan^{-1} 2$. The initial domain and grid set-up are the same as in the first example. The Riemann solution for this example contains two fast shocks and two rarefaction waves, a slow compound, a contact discontinuity, and a slow shock (see Fig. 4.3 for the numerical results). The errors of the three schemes (Roe's, MHD-HLLC, and HLL), calculated via Eq.(34), are 0.0250, 0.0218, and 0.0267 respectively. It is interesting to see that the MHD-HLLC solver is even more accurate than Roe's scheme for this problem.

4.2 Two-dimensional propagation of Alfvén wave

This example is taken from Ref.[6]. It is pointed out in Ref. [6] that some schemes that perform quite well for hydrodynamical tests may have difficulties with the propagation of Alfvén

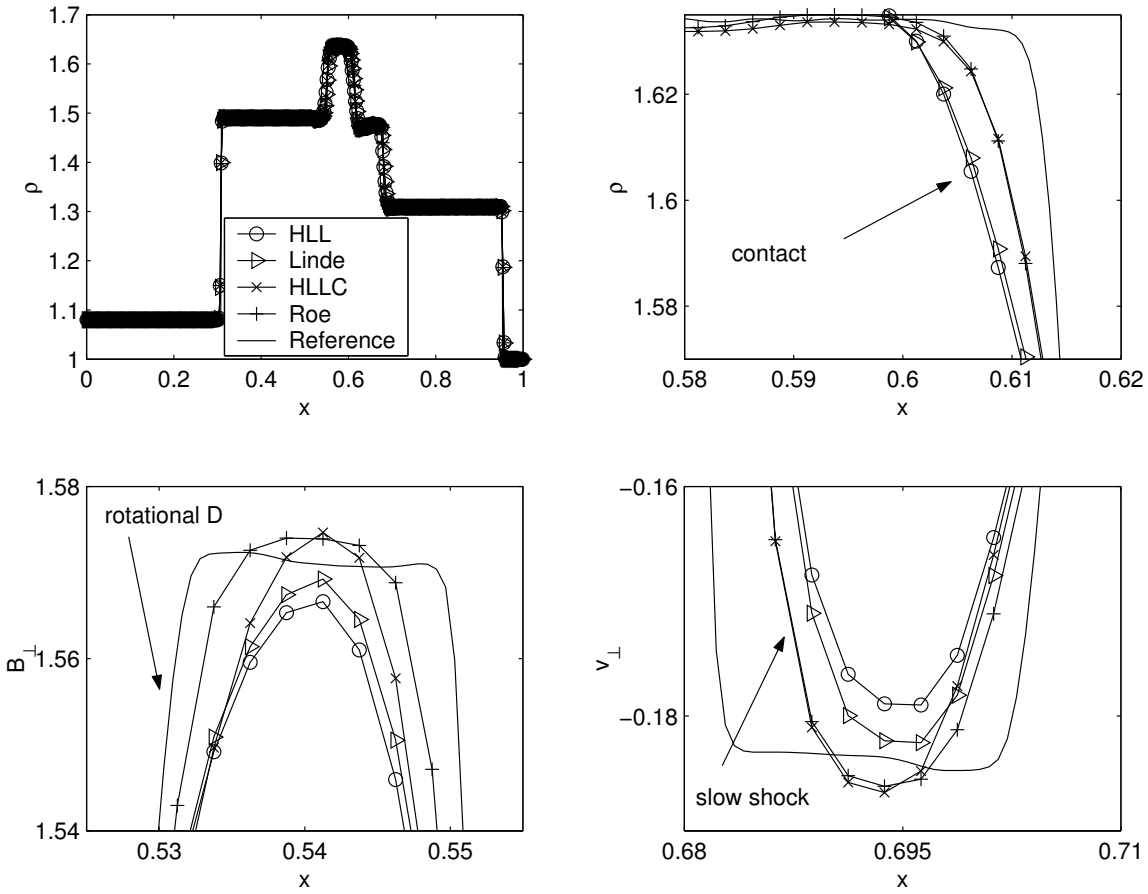

Fig. 4.1. Results for 2.5D shock-tube problem. The angle between the shock interface and y-axes is 0. Output is at $t = 0.2$.

waves. The set-up of the problem is as follows. A circular pulse of velocity perpendicular to the plane of computation is initialized at the center of a 200×200 zone grid which contains a uniform magnetic field. Throughout the plane, the density, pressure, and adiabatic index are set to 1, 3/5, and 5/3, respectively. The velocity is set to zero everywhere, except for a circular region in the center of the grid with a radius of 10 zones in which v_3 is set to 10^{-3}. In Ref.[6], the Alfvén pulse has been either transported in x-direction or in diagonal direction. We test the problem with a different propagation direction by setting the magnetic field as $B_x = 1, B_y = 2$. This problem has exact solutions for v_3. The circular pulse in v_3 should be carried along the magnetic field line at the Alfvén speed intact and undistorted.

We solve this example with three different Riemann solvers. Figs. 4.4-a and 4.4-c show the results of MHD-HLLC, Roe's, and HLL Riemann solver. It is clear that HLL Riemann solver is more diffusive than MHD-HLLC Riemann solver. For this example, HLL took 36 seconds, MHD-HLLC 38 seconds, and Roe's solver took 50 seconds.

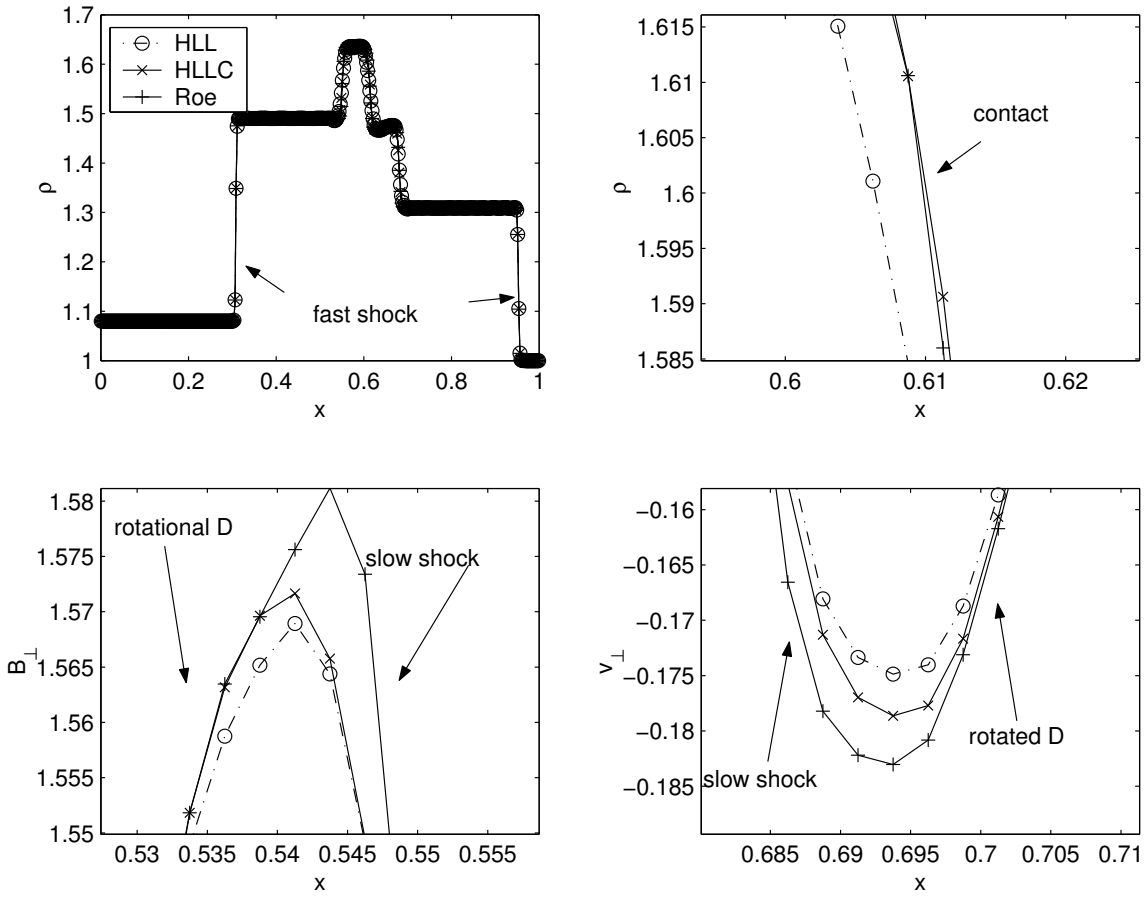

Fig. 4.2. Results for 2.5D shock-tube problem. The angle between the shock interface and y-axes is $\tan^{-1} 2$. Output is at $t = 0.2/\sqrt{5}$.

4.3 Rotor problem

This test problem is taken from Ref.[1]. It was also used by Tóth [22] to compare several numerical schemes. We use exactly the same set-up of the problem as was described in [22].

We solve the first rotor problem of Ref. [22] to time 0.15. It was reported by Tóth [22] that many one step TVD base scheme failed to solve this problem due to negative pressure. We did not encounter any difficulties with all of our solvers and time integration schemes. We used two-level refinement with refinement ratio of 3. Fig. 4.5 shows the results for Roe's, MHD-HLLC and HLL Riemann solvers. HLL solver took 34 seconds, MHD-HLLC solver took 37 seconds, and Roe's solver took 52 seconds to reach the final time $t = 0.15$. It is clearly seen that the HLL solver was too diffusive.

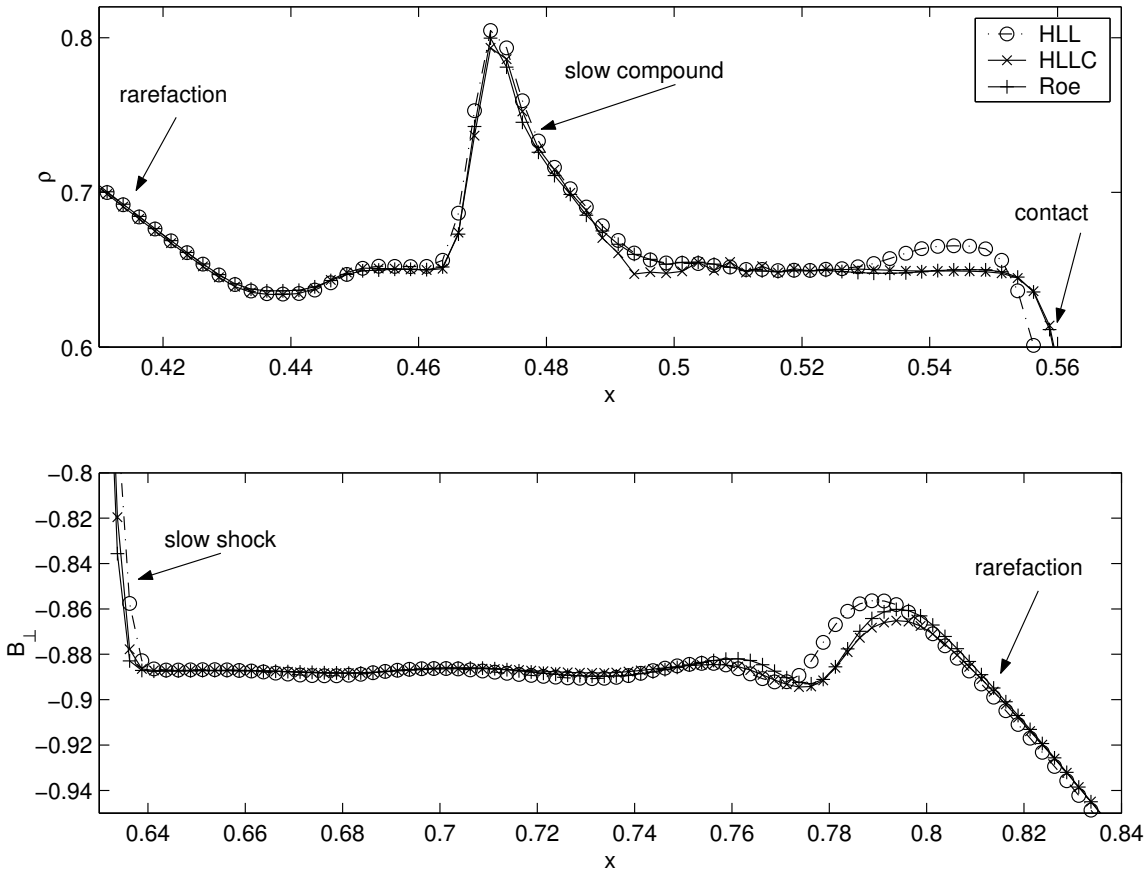

Fig. 4.3. Results for Brio and Wu's shock-tube. The angle between the shock interface and y-axes is $\tan^{-1} 2$. Output is at $t = 0.2/\sqrt{5}$.

5 Conclusion

We have extended the HLLC Riemann solver for HD equations to MHD equations. The new MHD-HLLC solver satisfies the integral form of conservation laws, does not require eigen-decomposition, and can greatly improve the computational efficiency for MHD problems. This method is an improvement over HLLE, and any one who uses a central scheme or ENO scheme based on either the Lax Friedrichs or HLLE flux can use the HLLC flux to improve their results for MHD calculation.

We acknowledge that despite the computational efficiency advantage, the new MHD-HLLC solver must inevitably be more diffusive on a seven-wave system than a linearized method which takes into account all intermediate states. We recommend using the Roe's solver if exact resolution of the additional waves are considered important.

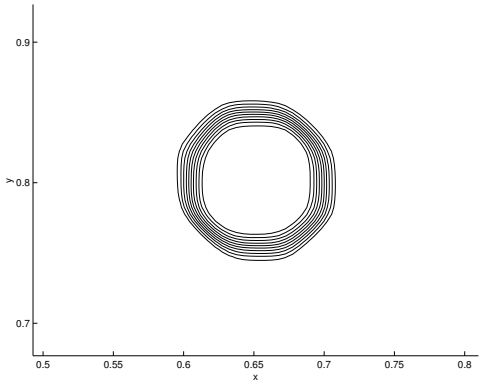

Fig. 4.4-a. Contours of velocity perpendicular to the grid (v_3) at $t = 0.15$. $B_x = 1, B_y = 2$. MHD-HLLC Riemann solver is used.

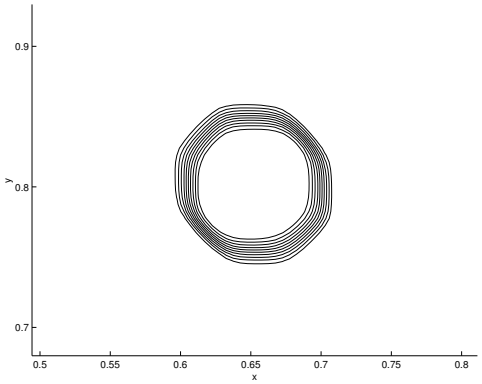

Fig. 4.4-b. Contours of velocity perpendicular to the grid (v_3) at $t = 0.15$. $B_x = 1, B_y = 2$. Roe's Riemann solver is used.

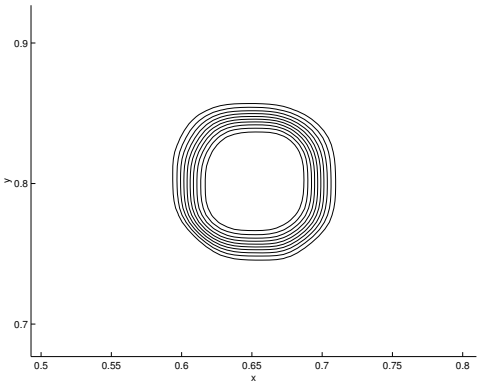

Fig. 4.4-c. Contours of velocity perpendicular to the grid (v_3) at $t = 0.15$. $B_x = 1, B_y = 2$. HLL Riemann solver is used.

Acknowledgements

We would like to thank Dr. H. Li for a careful reading of the manuscript and many useful discussions. We also thank Drs. T. Gardiner and J. Stone for helping test our new solver. This research was performed under the auspices of the Department of Energy. It was supported by the Laboratory Directed Research and Development (LDRD) Program at Los Alamos. It is also available as Los Alamos National Laboratory Report, LA-UR-03-8922. During the review process of this paper, we were notified of the recent work by Dr. Gurski ([11]), which contain similar results with ours for 1-D ideal MHD cases, though her approach and ours are very different.

References

[1] D. S. Balsara and D. S. Spicer, A staggered mesh algorithm using high order Godunov fluxes to ensure solenoidal magnetic fields in magnetohydrodynamics simulations, *J. Comput. Phys.*

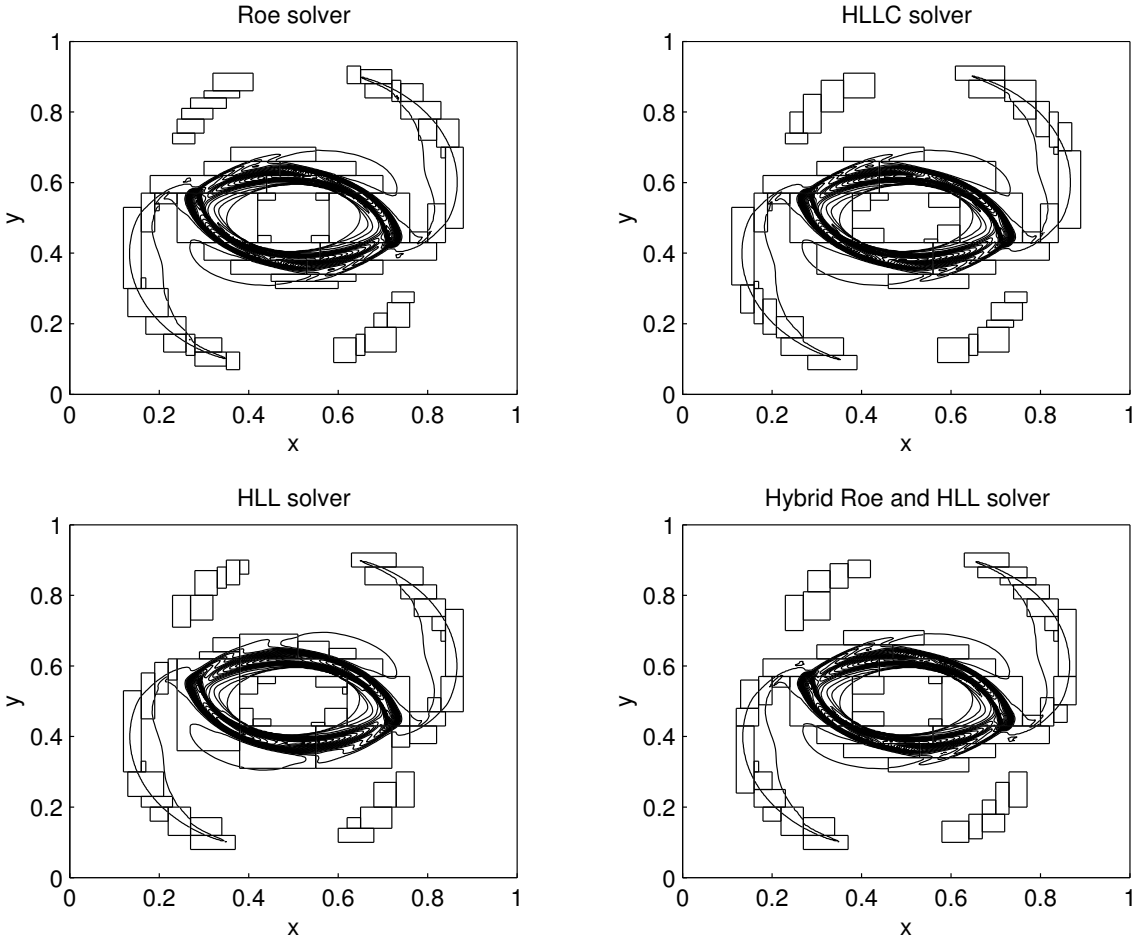

Fig. 4.5. Results for rotor problems with dimensional split solvers. 30 contours between 0.483 and 12.95 are used.

149 (1999), 270-292.

[2] D. S. Balsara, Total variation diminishing scheme for adiabatic and isothermal magnetohydrodynamics, *ApJS*, 116 (1998), 133.

[3] D. S. Balsara, Divergence-free adaptive mesh refinement for magneto-hydrodynamics, *J. Comput. Phys.*, 174 (2001), 614-648.

[4] P. Batten, N. Clarke, C. Lambert, and D. Causon, On the Choice of Wave Speeds for the HLLC Riemann solver. *SIAM J. Sci. Comput.*, 18 (1997), 1553-1570.

[5] M. Brio and C. C. Wu, An upwinding differencing schemes for the equations for ideal Magnetohydrodynamics, *J. Comput. Phys.*, 75 (1988), 400.

[6] D. A. Clarke, A consistent method of characteristics for multi-dimensional magnetohydrodynamics, *ApsJ*, 457 (1996), 291-320.

[7] W. Dai and P. R. Woodward, Extension of piecewise parabolic method (PPM) to multidimensional magnetohydrodynamics, *J. Comput. Phys.*, (111 (1994), 354.

[8] W. Dai and P. R. Woodward, A simple finite difference scheme for multidimensional magnetohydrodynamics, *J. Comput. Phys.* 142 (1998), 331-369.

[9] B. Einfeldt, On Godunov-type methods for gas dynamics, *SIAM J. Numer. Anal.*, 25 (1988), 294.

[10] B. Einfeldt, C. D. Munz, P. L. Roe, and B. Sjogreen, On Godunov-type methods near low densities, *J. Comput. Phys.*, 92 (1991), 273.

[11] K. Gurski, An HLLC-type approximate Riemann solver for ideal magneto-hydrodynamics, *SIAM J. Sci. Comp.*, 25 (2004), 2165-2187.

[12] A. Harten, P. D. Lax, and B. van Leer, On upstreaming differencing and Godunov-type schemes for hyperbolic conservation laws, *SIAM Rev.*, 25 (1983), 35.

[13] P. Janhunen, A positive conservative method for magnetohydrodynamics based on HLL and Roe methods, *J. Comput. Phys.* 160 (2000), 649.

[14] G. S. Jiang and C.-C. Wu, A high-order WENO finite difference scheme for the equations of ideal Magneto-hydrodynamics, *J. Comput. Phys.*, 150 (1999) 561-594.

[15] T. Linde, A practical general-purpose two-state HLL Riemann solver for hyperbolic conservation laws, *Int. J. Numer. Meth. Fluids*, 40 (2002), 391-402.

[16] S. Li and H. Li, A modern code for solving magnetohydrodynamics or hydrodynamic equations, Technical Report, Los Alamos National Laboratory, 2003.

[17] K. G. Powell, *An approximate Riemann solver for MHD (that actually works in more than one dimension),* Technical Report N0. 94-24, (ICASE, Langley VA, 19994).

[18] K. G. Powell, P. L. Roe, T. J. Linde, T. I. Gombosi, and D. L. DeZeeuw, A solution-adaptive upwinding scheme for ideal magnetohydrodynamics, *J. Comt. Phys.*, 154 (1999), 284.

[19] P. L. Roe, Approximate Riemann solvers, parameter vectors, and difference schemes, *J. Comput, Phys.*, 43 (1981), 357-372.

[20] P. L. Roe and D. S. Balsara, Notes on the eigensystem of magnetohydrodynamics, *SIAM J. Appl. Math.*, 56 (1996), 57.

[21] D. Ryu and T. W. Jones, Numerical magnetohydrodynamics in astrophysics: algorithm and tests for one-dimensional flow. *ApJ*, 442 (1995), 228-258.

[22] Gabor Tóth, The $\nabla \cdot B = 0$ constraint in shock-capturing magnetohydrodynamics codes, *J. Comp. Phys.*, 161 (2000), 605-652.

[23] E. F. Toro, Riemann Solvers and Numerical Methods for Fluids Dynamics, Springer, Berlin, Heidelberg, Second Edition, 1999.

[24] E. F. Toro, M. Spruce, and W. Speares, Restoration of the contact surface in the HLL-Riemann solver. *Shock Waves*, 4(1994), 25-34.

[25] M. Wesenberg, Efficient MHD Riemann solvers for simulations on unstructured triangular grids, *J. Numer. Math.*, 10 (2002), 37-71.

[26] A. L. Zachary, A. Malagoli, and P. Colella, A higher-order Godunov method for multidimensional ideal magnetohydrodynamics, *SIAM J. Sci. Comput.*, 15 (1994), 263.